Hartigan's Dip Test of Unimodality

Applied on Terrestrial Gamma-ray Flashes

By: Matthew Stanbro

Mentored by: Michael Briggs

Abstract:

Terrestrial gamma-ray flashes (TGFs) have been observed in association with thunderstorms. These events last in the time range of less than a millisecond at high altitudes. Varying amount of pulses has been observed during any one event with an unknown cause. Events have single, overlapping, and multiple pulses TGFs have all been detected. In order to separate each event into their corresponding pulse count, Hartigan's dip test is applied to 30 different TGFs found by the Gamma-ray Burst Monitor (GBM). The test checks for multi-modality by creating a dip statistic and also displays a modal interval. This dip statistic can then be compared to a chart to find the probability of multi-modality. To apply the dip test to TGFs, an accumulative subroutine is run to place the photon detection in ascending order, a requirement for the dip test. The dip statistic shows that most single pulse TGFs have a 5-10% chance to be multiple pulses, and clearly separated double pulses have a 50-90% chance. This is a slight problem since single pulses should have a probability closer to 50% and clearly separated pulses should have a probability around 90-99%. Another problem occurs with the dip test of overlapping pulses showing a probability of 5-10% of multimodality. This places it in the same range of probability as single pulses. The cause of the problems for single and overlapping pulses are believed to be because of the accumulative subroutine does not allow a steady mode to be within the data. The cause for a low probability of a double pulse is unknown. Due to these poor dip statistics, the dip test may not be capable of categorizing TGFs in this manner.

1. Introduction

The research done in this project is based off four basic areas. These areas are TGFs, Hartigan's dip test of unimodality, the GBM, and Fortran.

1.1. Terrestrial Gamma-ray Flashes

Terrestrial burst of gamma rays were first observed by the Burst and Transient Source Experiment (BATSE) instrument on the Compton Gamma Ray Observatory in 1994 (*Fishman et al.*, 1994). Each pulse of a TGF normally last less than a millisecond and have continued to be observed by the Reuven Ramaty High energy Solar Spectroscopic Imager (RHESSI) satellite (*Smith*, 2005), the GBM on the Fermi Gamma-ray Space Telescope (*Briggs et al.*, 2009), and other space telescopes. BATSE observed correlations with thunderstorms, which have been confirmed with RHESSI. This correlation occurs at regions above a thundercloud caused by lightning discharges or inside of thundercloud tops caused by lightning. One such argument for an origin above or inside the thundercloud tops is based on the distribution of TGFs. One can see the density of TGFs is small for areas around the Midwestern United States and the Mediterranean from Figure 3 in Smith's paper. Smith discusses that if one plots the efficiency of TGFs per lightning flash as a function of latitude, there is a drop off of TGFs rate near the latitudes around these points. This is speculated to be because TGFs created in mid-latitudes are not high enough to escape into space (*Fishman et al.*, 1994 and *Smith*, 2005).

The cause of gamma-ray flashes were actually predicted 2 years before the first gamma-ray was found by Gurevich. Gurevich proposed that relativistic runaway avalanches of electrons will cause an energy burst. The gamma-ray spectrum produced from such an event must have at least energy of 25

MeV. In order to achieve such a spectrum, Smith states three conditions are required: the field must be high enough for runaway electrons, the total potential drop must higher than several tens of MeV, and air density must be high enough to provide several electron collisions to occur in the field (*Smith*, 2005).

The first multiple pulse TGFs were also observed by BATSE. Events with two pulses observed by Fishman had peak separations from 1 to 4 milliseconds and multiple pulses with variable time spacing in milliseconds (*Fishman et al.*, 1994). GBM and the other instruments have confirmed these events by observing multiple pulses during the same event. The cause of multiple pulses to occur instead of a single pulse is still unknown.

Events have also been observed in which pulses overlap each other (*Briggs et al.*, 2010). Briggs was able to distinguish between overlapping pulses that are symmetrical by applying the Gaussian function on the event,

$$f(\mathrm{t}) = \frac{A}{\sqrt{2\pi}\sigma} \exp\left[-\frac{1}{2}\left(\frac{t-t_p}{\sigma}\right)^2\right], \quad (1)$$

that has free parameters amplitude A in counts per second, peak time t_p, and width σ both in seconds. For asymmetrical pulses, he applied a lognormal function,

$$f(\mathrm{t}) = \frac{A}{\sqrt{2\pi}\sigma(t-t_s)} \exp\left[-\frac{1}{2}\left(\frac{log\frac{t-t_s}{\tau}}{\sigma}\right)^2\right], \quad (2)$$

for $t > t_s$. This equation has free paramaters amplitude A in counts per second, start time t_s and timescale τ both in seconds, and shape σ. Both of these functions can be found in his paper and discussed more in detail (*Briggs et al.*, 2009).

With all this knowledge of TGFs, there are still many questions unanswered about these events. TGFs are relatively new, only being found over 15 years ago. Some of these questions are why some events have a single pulse and other have multiple pulses and are TGFs the initiation mechanism of the associated lightning or a byproduct of the lightning. Smith believes with the new missions and current missions we will be able to answer questions such as these (*Smith*, 2009). In an effort to categorize TGF events by if they are multiple pulses, overlapping pulses, or a single pulse, Hartigan's dip test of unimodality is applied on multiple events instead of the two equations Briggs used.

1.2. Hartigan's Dip Test of Unimodality

Hartigan's dip test checks if statistical data has more than one mode in its distribution. The test is made by Hartigan, J. and Hartigan, P. The test creates a unimodal distribution function that has the smallest value deviations from the empirical distribution function. The largest of these deviations is the dip statistic. The dip statistic tells you the probability of the empirical distribution function being bimodal. By having a large value dip, the empirical data is more probable to have multiple modes (*Hartigan et al.*, 1985).

The test considers n(n-1)/2 possible modal intervals (X_L , X_U) within the data. It then creates the greatest convex minorant (gcm) and least concave majorant (lcm) of the empirical distribution function

TABLE 1
Percentage points of the dip in uniform samples

(1) *Dip is the maximum distance between the empirical distribution and the best fitting unimodal distribution.*
(2) *Based on 9999 dips. Maximum standard error is* .001.

sample size	probability of dip less than tabled value is								
	.01	.05	.10	.50	.90	.95	.99	.995	.999
4	.1250	.1250	.1250	.1250	.1863	.2056	.2325	.2387	.2458
5	.1000	.1000	.1000	.1217	.1773	.1872	.1966	.1981[3]	.1996[3]
6	.0833	.0833	.0833	.1224	.1586	.1645	.1904	.2034	.2224
7	.0714	.0714	.0822	.1181	.1445	.1597	.1832	.1900	.2035
8	.0625	.0745	.0828	.1109	.1428	.1552	.1744	.1801	.1978
9	.0618	.0735	.0807	.1041	.1362	.1458	.1623	.1693	.1851
10	.0610	.0718	.0780	.0979	.1302	.1394	.1623[3]	.1699	.1828
15	.0544	.0606	.0641	.0836	.1097	.1179	.1365	.1424	.1538
20	.0474	.0529	.0569	.0735	.0970	.1047	.1209	.1262	.1382
30	.0395	.0442	.0473	.0617	.0815	.0884	.1012	.1061	.1177
50	.0312	.0352	.0378	.0489	.0645	.0702	.0804	.0842	.0926
100	.0228	.0256	.0274	.0355	.0471	.0510	.0586	.0619	.0687
200	.0165	.0185	.0197	.0255	.0341	.0370	.0429	.0449	.0496

(3) *Repeated computations.*
(4) *Interpolate on* $\sqrt{n}$ *dip.*

Reprinted from "The Dip Test of Unimodality" by J. A. Hartigan and P. M. Hartigan, 1985, *The Annals of Statistics*, 13.

in interval ($-\infty$, X_i) and (X_j , ∞).If d_{ij} is the maximum distance between the empirical distribution and these two curves, then twice the dip is the minimum value of d_{ij} over all modal intervals (X_i , X_j).The dip is then compared to Table 1 from Hartigan's paper. In Table 1, n is the sample size, and the top portion is the probability that the dip is bimodal. To get the probability data, Hartigan calculated the dip 9,999 times on uniform data with varying sample sizes n. From Theorem 3 in Hartigans' paper, the dip can be interpolated to varying sample sizes based on the $\sqrt{n} * DIP$ (*Hartigan et al.*, 1985).

The dip test was compared against the likelihood ratio test and the depth test to test their power. This comparison found that the dip test had a better chance of finding unimodality then both of these test. The only knowledge one needed to find the dip is the data input in ascending order, while the likelihood ratio requires more input and the depth takes longer to complete. For these reasons, we choose the dip test as our test instead of these two tests (*Hartigan et al.*, 1985).

1.3. Gamma-ray Burst Monitor

All data obtained for this research is from the GBM. The satellite consists of two instruments to observe gamma-rays, The Large Area Telescope and the GBM. These instruments are arranged to cover sky with nearly uniform sensitivity. The GBM obtains data by a triggering process that is turned on by a significant rate increase in photon detection. Once this increase is detected, GBM's software turns and saves the detection as a time-tagged event (TTE) (*Briggs et al.*, 2010). Because of this triggering mechanism, GBM detects approximately 2 events per week. While this trigger mechanism is useful for

finding strong pulse TGFs, it misses some of the weaker TGFs that RHESSI can find by doing calculations on the ground. For a portion of Fermi's orbit, it also provided a technique to detect TGFs similar to RHESSI, but this data is still being reviewed (*Fishman et al.*, 2011).

A weakness of this triggering mechanism is the time window the GBM has to detect a TGF. Due to GBMs onboard hardware limitations, the time window for a GBM trigger is 16 milliseconds. This reduces the amount of TGFs detected by GBM since most TGFs are only a fraction of a millisecond long. This large time window has to include background noise from other sources along with a TGF (*Fishman et al.*, 2011).

Once a TTE is observed, it is stored as a Flexible Image Transport System (FITS) file in the National Aeronautics and Space Administration's (NASA) GBM database. These files are the most commonly used digital file format in astrophysics. This file format support many programming languages. The read TTE data is used to read this type of file and allows for easy accessibility to GBM's data. The public database used by NASA is where all TGF data is pulled.

1.4. Fortran

The program in this report will be programmed in Fortran. Fortran was officially standardized in 1966 by the American Standards Association, known as FORTRAN 66. Over the years, Fortran evolved into FORTRAN 77, Fortran 90, and Fortran 95. With every new iteration of Fortran came new standardization of programming along. Fortran 90 standard not only help standardize practices, but it introduced features new to Fortran found in other languages (*Metcalf et al.*, 2004).

In Fortran 95, outdated features from the previous iterations of Fortran were deleted. While there were compliers still around, this provided a new standard of programming instead of using outdated features (*Metcalf et al.*, 2004). Since Fortran is in use in so many programs today by NASA and other academia, Fortran will be the primary language used create to create the dip test. Along with Fortran, the UNIX language will is used. This language also heavily influences the scientific community and is an easy choice for languages of this report.

2. TGF Dip Test Program

The program to test a TGF event is separated into a main program that holds 3 main subroutines. These subroutines read the TTE event, accumulate the photon detection, compute the dip statistic, and graph the accumulated array. The main program and read TTE subroutine is provided by Briggs. The main program is a histogram plotting program that has been heavily altered to create the TGF Dip Test Program. A histogram plotting program is chosen as the main program, so the accumulated data can be easily translated to an accumulative histogram plot.

The program is first complied using a .sh file. This file contains the UNIX command line that needed to compile all subroutines and main program. The command must create the read TTE subroutine and DipTest subroutine in a separate line than the main program. This is because the read TTE subroutine is in C language and the DipTest subroutine is in FORTRAN 77 unlike the main program. The main program is written in Fortran 95.

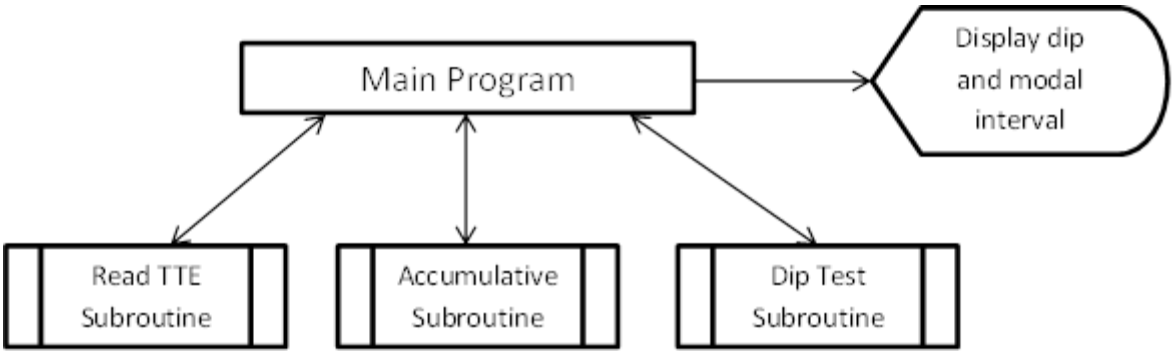

Figure 1: Program Flow Chart

The program works in a fashion shown in Figure 1. The main program asks for user input and then calls the read TTE subroutine. This subroutine returns back to the main program and then the main program calls the accumulation subroutine. Again, this subroutine returns to the main program with the dip statistic and modal interval. The main program then displays the dip and modal interval from the dip test subroutine. After more user input, the main program also displays a plot of the accumulated counts per bin width in microseconds versus time range relative to trigger time in milliseconds.

2.1. Read TTE Subroutine

Since the TTE event is stored as a .fit file extension, a subroutine is called to read the TTE event and store it. This code reads the data based on a time range in milliseconds and a bin width in microseconds. The code reads from all 14 GBM detectors in this time range and bin width to place the amount of photons detected in a global array (GBL_DATA) available to all subroutines. It is important to select the correct time range and bin width. By choosing a bin width too small, the intensity of the pulse will be similar to that of the background noise. If a bin width is chosen to be very large, a small sample size is obtained, and the background noise is included with the intensity of the TGF. Another note to take when running the program is that the .fit file must be inside the same folder that the program is run in.

2.2. Accumulation Subroutine

Hartigan's dip test requires the data input to be in ascending order. Since the TTE event is read based on time, photon detection varies based on time. An accumulation subroutine was created to place the photon detection in an increasing order as time progresses. This subroutine creates an additional array (ACCUM) with the new accumulated values. This allows the dip test code to run within its restrictions without altering the dip test code. The accumulation subroutine works in the following 3 steps.

(1) Place GBL_DATA(1) into ACCUM(1).
(2) ACCUM(i) = DATA(i) + ACCUM(i-1)
(3) Repeat step (2) from i=2 to i=n, where n is the last value in array GBL.

2.3. The Dip Test Code

The original dip test code in Hartigan's paper had an error in it. In order to avert the error, F. Mechler's 2002 modified dip test code was chosen. His modified code checks for a perfectly unimodal data, which previously gave an infinite cycle. It also fixes the error in the original code where a ')' was misplaced. The misplaced ')' gave a larger dip value than expected (*Mechler*, 2002). Mechler's code was altered to read the TGF data and be used by the main program.

Hartigan's code is run in several steps. The first step sets X_L = ACCUM(1) and X_U = ACCUM(N), where 1 is the first data input in the ACCUM array and N is the last value in the array. It also sets the DIP = 0. It then establishes the indices in which the lcm and gcm fit. Afterwards, the code begins to cycle through the data to find the change points for the gcm and lcm. It finds the gcm change points from high to low and the lcm change points from low to high. The code then finds the largest distance greater than 'DIP' between the GCM and LCM from low to high. The DIP is then computed from the gcm and lcm and recycles through the program until the best value dip is found. Once this dip is found, it is halved and saved as dip of the interval. These steps can be found inside Mechler's code (*Mechler*, 2002).

The dip test code also provides errors indicators in case the dip test could not run properly. There are 4 different fault indicators to alert you of any errors. A fault indicator of 0 means the dip test was successfully executed and is the indicator one is looking for. A fault indicator of 1 means no sample size was given and a fault indicator of 2 means the data is not in ascending order (*Hartigan*, 1985). These two faults should never be given in the program, but fault indicator 5 may be. This indicator was added by Mechler. Fault indicator 5 means the inputted data is perfectly unimodal and cannot display a dip because an infinite loop will occur. This indicator breaks that loop (*Mechler*, 2002). If this fault is encountered, the time range needs to be extended or a different bin width chosen to allow a larger deviation away from a perfectly unimodal curve.

This code was tested with the example in Hartigans' paper. This example has the quality of faculty in 63 statistics departments. When this data was inputted into the dip test code, it had a dip statistic of .059. From Table 1 one can find the probability of bimodality of this value to be 90%. This corresponds with what is found in the paper which they find a tail probability of 10% (*Hartigan et al.*, 1985).

3. Results of TGFs

Several events with known TGFs were tested for unimodality with the TGF dip test program. These TGFs were found in Fishman's paper that sourced 53 different TGF pulses. 30 different TGF that included single pulses, double pulses, and overlapping pulses were ran through the program to find their dip statistic. Some of their plots from Fishman's paper and accumulation plots can be found in Figure 2-4 on pages 13-16. All TGFs time ranges are relative times based off the trigger time of the event the time ranges chosen to analyze each TGF is the start of the first pulse and end of the last pulse. The start and end time of the pulses are found from Fishman's paper in 2011. The time started is roughly .02

Table 2: Single Pulse TGFs Dip Statistic and Probability

TGF #	BN# V#	TIME INTERVAL	BIN WIDTH	SAMPLE SIZE	DIP	PROBABILITY OF BIMODALITY
1	080828449 01	-11.53 -11.38	20	8	0.0744	5.0%
2	081001392 04	-12.96 -12.8	20	9	0.0611	1.0%
3	081006797 01	-0.95 -0.79	20	8	0.0643	1.0%
4	081025691 01	-9.72 -9.57	20	8	0.0682	1.0%
5	081123874 01	-10.34 -10.2	20	8	0.0664	1.0%
6	090510498 00	-2.32 -1.38	80	12	0.0472	1.0%
7	091118985 00	-2.38 -2.25	20	7	0.0915	10-50%
8	091130219 00	-15.5 -15.39	20	6	0.115	1-50%
9	091213876 00	-4.22 -4.11	20	6	0.0855	1-50%
10	091221677 00	-8.19 -8.02	20	9	0.0977	10-50%
11	091227801 00	-4.66 -4.46	20	11	0.0501	1.0%
12	100125883 00	-12.79 -12.63	20	8	0.0833	10-50%
13	100202802 00	-0.27 -0.17	20	5	0.11	1-50%
14	100203793 00	-13.91 -13.68	20	12	0.0667	1-5%
15	100207843 00	-1.24 -1.09	20	8	0.0788	5-10%
16	100208349 00	-14.65 -14.52	20	7	0.0863	10-50%
17	100214868 00	-10.93 -10.78	20	9	0.0774	5-10%
18	100218518 00	-1.84 -1.7	20	8	0.0772	5-10%
19	100225374 00	-1.32 -1.19	20	7	0.0909	10-50%
20	100304842 00	-10.17 -10.05	20	7	0.0924	10-50%
21	100331421 00	-14.59 -14.44	20	8	0.0838	10-50%
AVG	N/A	N/A	N/A	8.142857143	0.0794381	5-10%

milliseconds before relative time in Table 2 of his paper. The end time is found by taking his pulse count in the same table and adding a few hundredths of milliseconds to it (*Fishman et al.*, 2011). This is done again until a drop off of photon detection occurs. By choosing the correct time range, all counts of photons will be found within the time range with the least amount of background interference.

3.1. Single Pulse TGFs

21 single pulse TGFs were run through the TGF dip test program. This data is found in Table 2 which displays the different dip statistics and probability of bimodality. The majority of these pulses were taken at a bin width of 20 microseconds besides TGF 6 taken at 80 microseconds. Figure 2 also shows a handful of these TGFs plots along with their accumulated data plots.

Checking the data from Table 2, one finds the average dip statistic is .07943 with a sample size of 8. This places the majority of the single pulses with the probability values to be bimodal to be 5-10%.

Table 3: Double Pulse TGFs Dip Statistic and Probability

TGF #	BN# V#	TIME INTERVAL	BIN WIDTH	SAMPLE SIZE	DIP	PROBABILITY OF BIMODALITY
22	081113322 01	-1.44 -.04	20	70	0.0485	50-90%
23	090627274 00	-21.3 -12.25	40	227	0.0236	50-90%
24	091224757 00	-2.22 -0.67	20	78	0.0491	50-90%
AVG	N/A	N/A	N/A	125	0.0404	50-90%

Roughly a third of the single pulse TGFs have a probability of bimodality of 1%, while another third has a probability greater than 10%. While this value is somewhat high for a single pulse, some of this error comes from the data. TGF 7 has a lot of variations around it is peak even though it is believed to be a single pulse. These variations will pull a high probability of bimodal due to the multiple dips in the data. TGF 12 also gets the same effect, but may also be influenced by how long pulse is. The pulse is a steady, relatively flat curve that is hard to determine where the peak of the data is located.

Two TGFs have a probability of bimodality range of 1-50%. TGF 13 gets this probability due to only having a sample size of 5. Checking back to Table 1, a sample size of 5 provides the same dip statistic for multiple probabilities. The sample size can be increased by taking a smaller bin width, but then the photon detection of the TGF is hard to separate from the background noise. TGF 8 and 9 also get a similar problem as TGF 13. Although they have a bin width of 6, it is still too small. The dip statistic does not begin to change for low probability until a sample size of 7 and 8 is reached.

Besides TGF 7 and 12, there are 5 other TGFs with a probability of bimodality range of 10-50%. TGF 10 is a long TGF believed to be due to electron beams. The length and low intensity of this TGF is similar to TGF 7. The other TGFs are hard to tell what exactly gives this high probability, but probably result from a similar phenomenon as the others.

3.2. Separated Double Pulse TGFs

Three separated double pulses TGFs were run through the program. The data and outcome can be found in Table 3. Their average dip statistic and sample size is .0404 and 125 respectively. This falls close to 70% of probability of bimodality which is quite low for clearly separated pulses. The bin width chosen for the double pulses are 20 microseconds besides TGF 23. It was chosen at a bin width of 40 due to time between pulses and low intensity of the first pulse. TGF 24 also contains an overlapping pulse as its second pulse. This pulse is analyzed in the overlapping TGFs data. This could possibly explain the higher dip value than the other 2 TGFs. Figure 3 shows all 3 of these TGFS plots and their accumulated data. The histogram plot of the TGF is from Fishman's paper.

3.3. Overlapping TGFs

Seven overlapping pulses TGFs were also ran through the program. Table 4 displays the outcomes of each of these events. The overlapping pulses have an average dip statistic of .07258 with

Table 4: Overlapping Pulse TGFs Dip Statistic and Probability

TGF #	BN# V#	TIME INTERVAL	BIN WIDTH	SAMPLE SIZE	DIP	PROBABILITY OF BIMODALITY
25	081223051 02	-12.22 -12.04	20	10	0.0725	5.0%
26	090522190 00	-6.42 -6.12	20	15	0.0522	1.0%
27	090808739 00	-13.12 -12.93	20	10	0.0554	1.0%
28	090828147 00	-10.13 -9.92	20	11	0.0639	1.0%
29	091213945 00	-12.24 -12.08	20	9	0.0677	1.0%
30	100110328 00	-10.47 -10.34	20	7	0.1087	10-50%
31	090627274 00	-12.4 -12.25	20	8	0.0877	10-50%
AVG	N/A	N/A	N/A	10	0.0725857	5-10%

an average sample size of 10. This places the probability of bimodality from Table 1 to be the same as single pulse TGFs or 5-10%. Over half of these pulses have a probability of bimodality of 1% which is more than the percent of single pulse TGFs.

TGF 30 and 31 have the highest probability of the 7 overlapping pulses. TGF 30 and 31 both contain a strong pulse and a weak pulse barely overlapping each other. One would also expect TGF 27 to share a similar characteristic as the other two, but the time range of this TGF may not be long enough to include the second pulse of this event. TGF 30 has a strong intensity pulse followed by a weak pulse, while TGF 31 has a weak pulse followed by a strong one. Besides the pulses barely overlapping and a weak pulse involved, the order of the pulse should not affect the value of the probability. Figures 4 show these 3 overlapping pulses and their accumulated data plots along with TGF 29.

4. Discussion

Discussion will be based around the TGF plots and the dip test using the tables. In the dip test section, possible errors for the erroneous probabilities are discussed as well as what future testing.

4.1. TGF Plots

The TGF plots display the accumulated data over time within the chosen bin width in microseconds in the y axis. The x axis displays the time range relative to the trigger time. Below the x axis is the trigger time. The y axis end point is chosen to be 50 counts above the greatest value in the accumulation table. Most of the graphs bin widths are 20 microseconds. This is different than the normal plots displayed by Fishman's paper which have a count of 10 microseconds. Fishman's plots have also been modified to display the TGF # displayed in this paper as opposed to the # assigned by him (*Fishman et al.*, 2011).

Comparing Figures 2, 3, and 4, one can already distinguish which pulses are clearly separated double pulses. However, comparing Figure 2 and 4, one begins to have some difficulty in distinguishing if the TGF is an overlapping TGF or a single pulse TGF. Both single and overlapping pulses linearly climb to the end of the plot and have a flat ending. This is because the time range is chosen to include the entire

pulse and not just the peak. From just observing the plots of single and overlapping TGFs one might see a problem with the technique of accumulating the data over the entire time, and the dip test results also show this same problem.

4.2. Dip Test

In the testing of the dip test using Hartigan's example, the dip test runs correctly, and it seems to work well within the single and double pulses as well. However, comparing Table 2 and Table 4 the dip test cannot currently distinguish the difference between a single and overlapping TGF. From these tables, both average probability of bimodality range 5-10%. This places the majority of overlapping pulses as single pulses. TGF 30 and 31 are the only TGFs with a probability higher than 10%. However, a third of the single pulse TGFs have the same probability and still causes the same problem. The program needs to be able to distinguish between these two to make it more efficient than the Gaussian and lognormal techniques used by Dr. Briggs.

The single pulse TGFs with a high probability is also a problem. While these high probabilities have been discussed in the results, it still poses a problem with distinguishing different types of pulses. Probabilities above 10% could be tested by the 2 equations used by Briggs, but then 90% of overlapping pulses would be missed and over a third of single pulses would be unnecessarily analyzed. This leads to a question is the dip test the correct test to use to categorize different TGFs.

Not only do the single pulse TGFs have a high probability, but the clearly separated double pulses have a probability of bimodality of 50-90% while clearly being two pulses. While it is much greater than single pulses' probability, one would expect the probability to be at 90% or greater. The reasoning for this low probability is unknown and needs to be further tested. The only possible solution is the dip test is looking for multiple modes, and the only mode available is the mode in between both pulses. Although the probability is lower than expected, comparing the overlapping pulse and the double pulse probability, the double pulse is much greater than the overlapping pulse and not equal. The two should be similar since they both have two pulses. With both the single pulse probability being the same as the overlapping pulse probability and the double pulse probability being greater than the overlapping's, there must be an error somewhere or the dip test does not work here.

One of these possible errors could be the time range chosen. Of course, if a pulse isn't found in the time range at all, one will know the dip statistic is just from background noise. But, if we choose a time range that includes the pulse and a lot of background noise, one may still find the unimodality or multimodality of a TGF. By analyzing the same TGFs found in Table 2-4 but at a range of 10 milliseconds before the event, one finds completely different probability for each TTE. The majority of the single TGFs will have 1%, but the error occurs where the modal interval is taken. All of the modal intervals in the TGFs analyzed this way will be at the very start of time range. This is because there is a very large mode there compared to anywhere else. By placing 5 milliseconds before and after the pulse, the probability of bimodality will almost always be greater than 90% because of the two modes before and after each event. Because of this limiting time range, the time range chosen in the paper is right before the first

pulse and directly after the last pulse. This helps eliminate any error from modes before or after the pulse.

With the time range error ruled out, there could be a possible error in the code. In order to eliminate this possible error, testing needs to be done on overlapping pulses that are similar to TGF 31. This test will create artificial exaggerated overlapping pulses that dip very close to the background noise, but have very high peaks. The dip test will hopefully catch this dip as a mode and give a probability of bimodality similar to the double pulses. If the test proves that the dip test can distinguish between the exaggerated pulses, then the dip test will not be able to be used to distinguish overlapping pulses like our data shows. If the test cannot distinguish the exaggerated pulse, we much look for another possible reason that the dip test gives such a small probability for overlapping pulses. One other such possible reason for a failure is the accumulation of the data.

If the test fails a possible reason for such erroneous probabilities may be because of the accumulation of the data. This is the main belief for failure of the dip test from comparing the plots of overlapping and single pulse TGFs. The reason that the accumulation of the counts may produce an error is because how the dip test works. The dip test is searching for a mode of data or data that is very close to the same value. This mode is created from a dip in the data value. For example, the double pulses have only noise background in between each pulse, so the accumulation of this data will lead to the same repeating number in between pulses. On the other hand, the overlapping pulses never reach the background noise in between pulses, so the accumulation of the data is always increasing. Looking at the accumulated plots in the figure section, one can see that the slope of the data is almost perfectly straight. This is similar to stating there are no modes or the data is perfectly unimodal. Due to the dip test requiring data in ascending order, the dip test may not work for the data if the accumulation of the data is at fault. Unless an alternative method can be found to create the TGFs counts in ascending order, the dip test will not be capable of categorizing the TGFs by their corresponding pulse traits.

5. Conclusion

In conclusion, the dip test failed to categorize TGFs by how many pulses they have. The main source of error is the lack of distinguishing overlapping TGFs from single pulse TGFs. Once further testing is done on the code to check if it is suitable for overlapping pulses calculation, we can check if probable error is the accumulation of the data. This is most likely the true error involved in the dip test causing an inaccurate dip statistic for overlapping TGFs. This is because the accumulated data is very close to linear and is hard to find multiple modes. Due to this problem, the dip test seems to not be capable of categorizing TGFs by their pulses. While the result of the test is not what we hoped for, it was worth doing the experiment to have faster means in categorizing TGFs.

6. Acknowledgements

I would like to thank Michael Briggs for the help throughout this project and reviewing this report. It has been a very beneficial experience to work with him as my mentor. I would also like to thank G. J. Fishman for providing the histogram plots of the TGF.

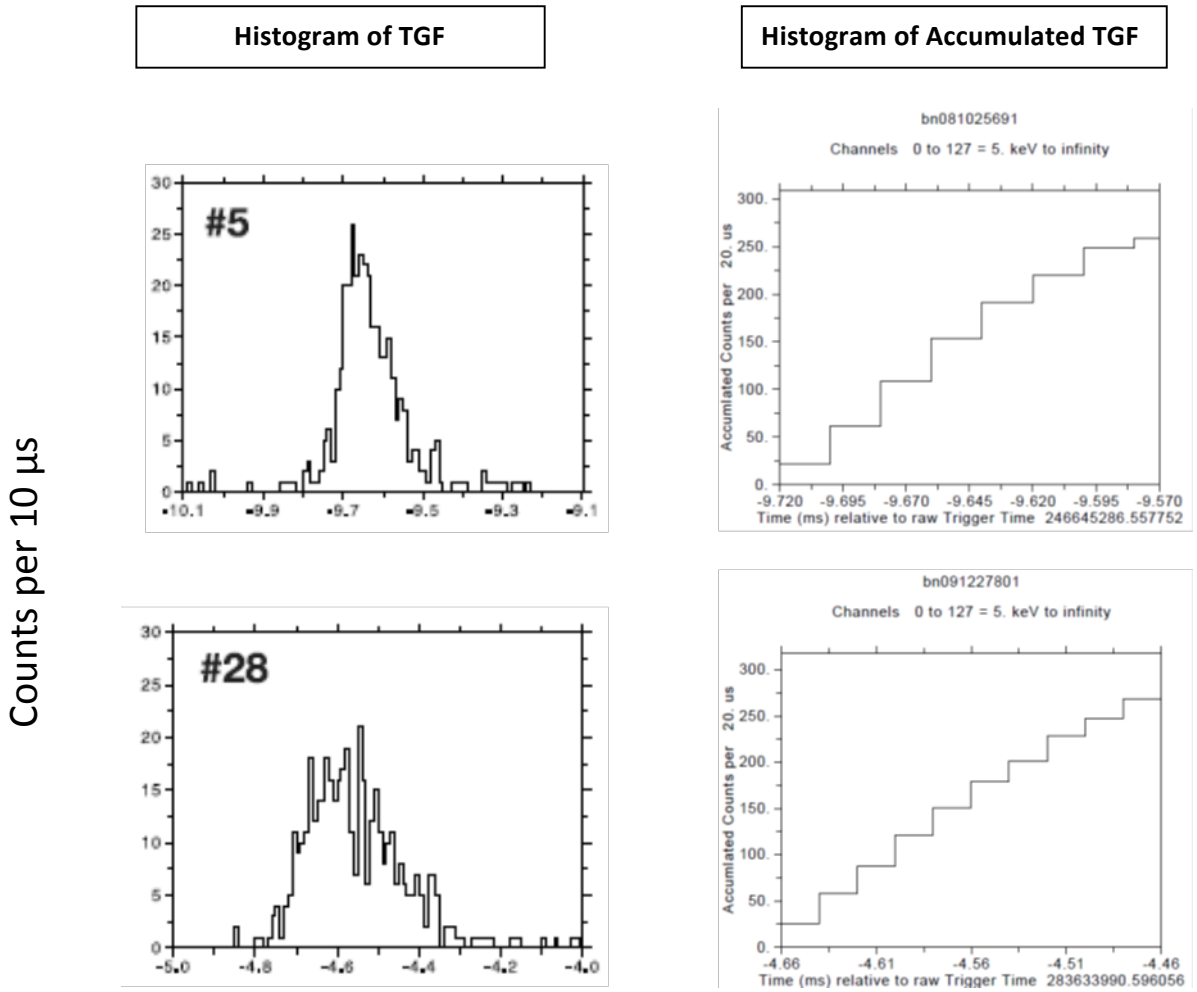

Figure 2: Single Pulse TGFs and Accumulation

Reprinted from "Temporal properties of the terrestrial gamma-ray flashes from the Gamma-Ray Burst Monitor on the Fermi Observatory" by G. J. Fishman *et al*, 2011, *Journal of Geophysical Research*, 116.

Histogram of TGF | **Histogram of Accumulated TGF**

Counts per 10 µs

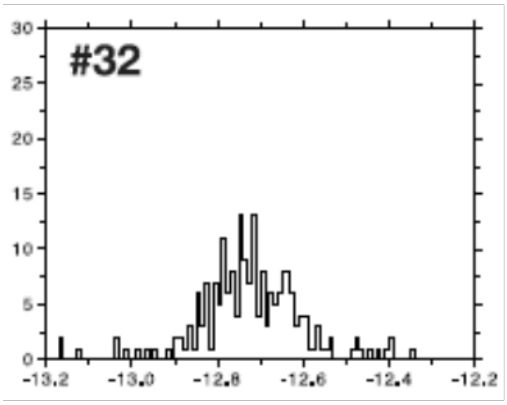

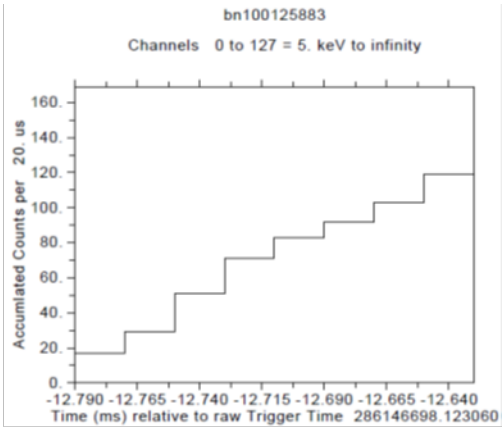

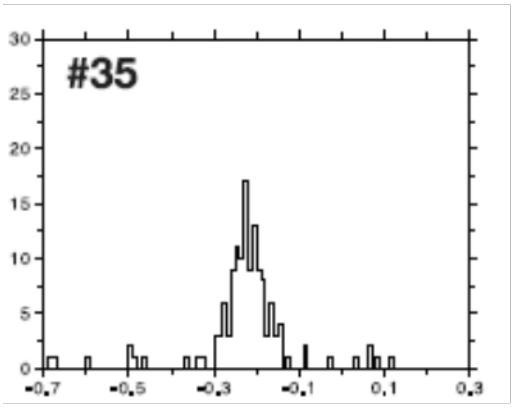

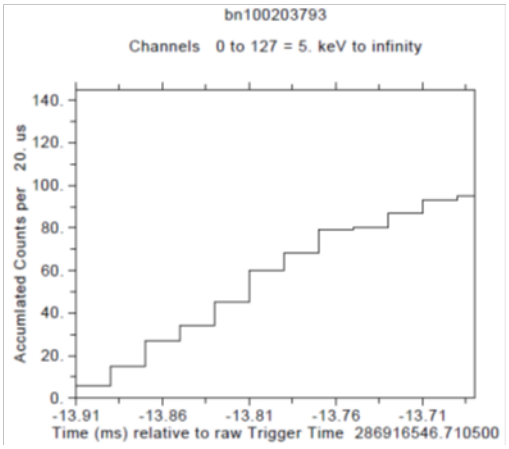

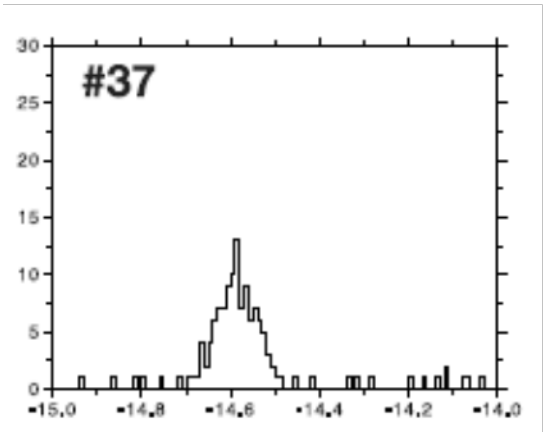

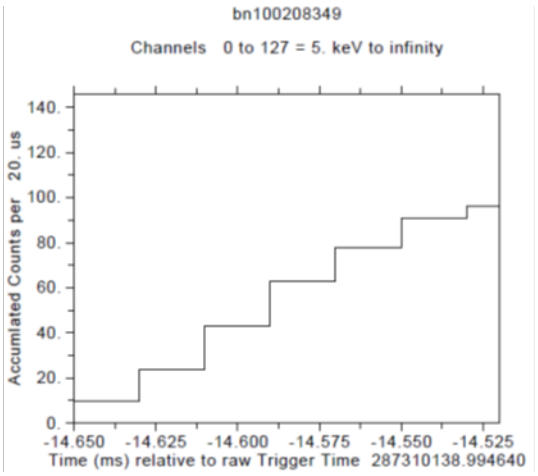

Figure 3 (Continued)

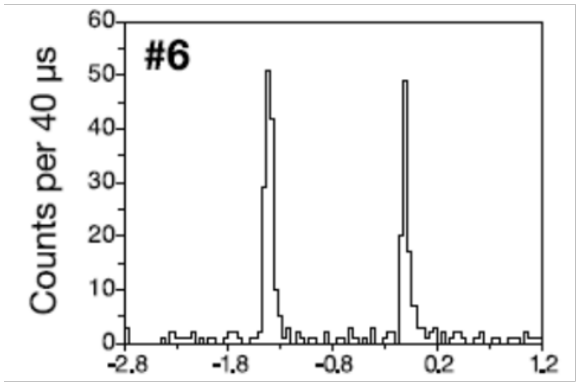
#6
Counts per 40 µs
60
50
40
30
20
10
0
-2.8
-1.8
-0.8
0.2
1.2

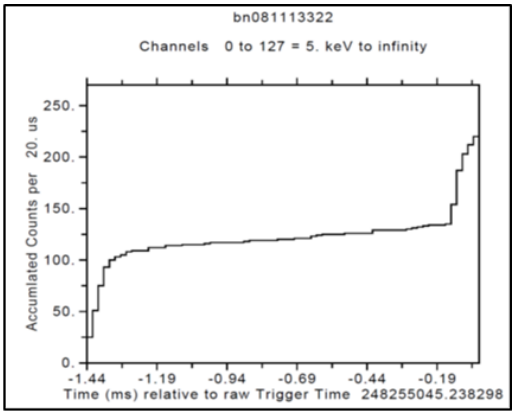
bn081113322
Channels 0 to 127 = 5. keV to infinity
Accumulated Counts per 20. us
250.
200.
150.
100.
50.
0.
-1.44
-1.19
-0.94
-0.69
-0.44
-0.19
Time (ms) relative to raw Trigger Time 248255045.238298

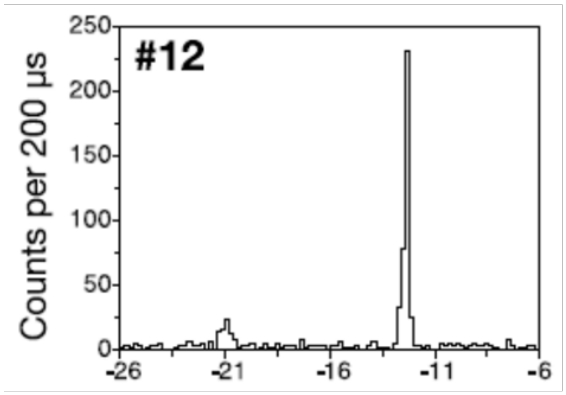
#12
Counts per 200 µs
250
200
150
100
50
0
-26
-21
-16
-11
-6

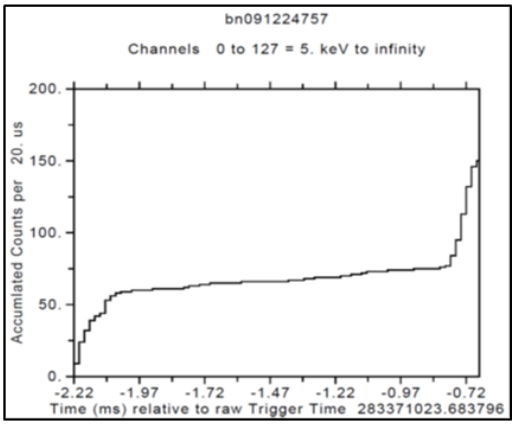
bn091224757
Channels 0 to 127 = 5. keV to infinity
Accumulated Counts per 20. us
200.
150.
100.
50.
0.
-2.22
-1.97
-1.72
-1.47
-1.22
-0.97
-0.72
Time (ms) relative to raw Trigger Time 283371023.683796

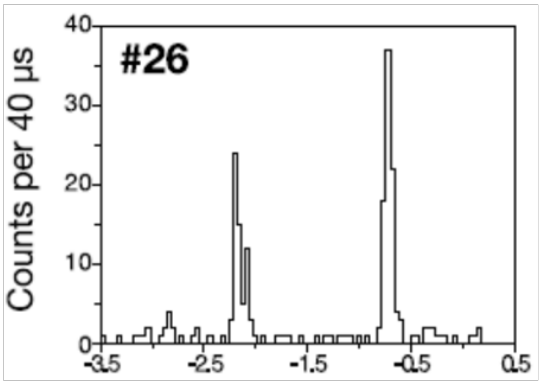
#26
Counts per 40 µs
40
30
20
10
0
-3.5
-2.5
-1.5
-0.5
0.5

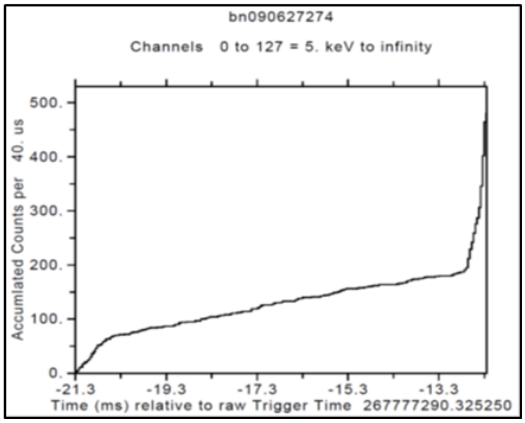
bn090627274
Channels 0 to 127 = 5. keV to infinity
Accumulated Counts per 40. us
500.
400.
300.
200.
100.
0.
-21.3
-19.3
-17.3
-15.3
-13.3
Time (ms) relative to raw Trigger Time 267777290.325250

Histogram of TGF **Histogram of Accumulated TGF**

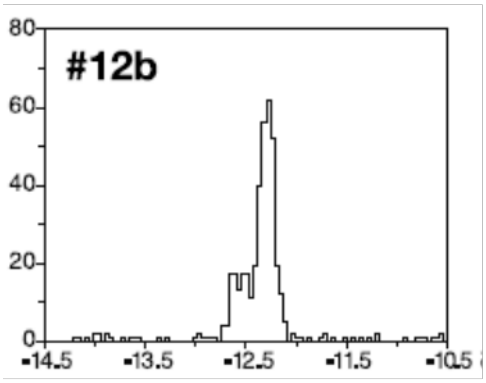

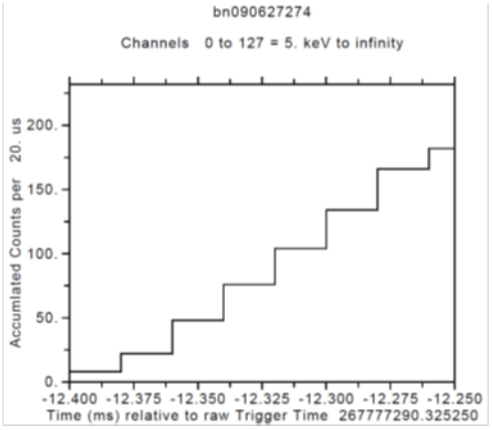

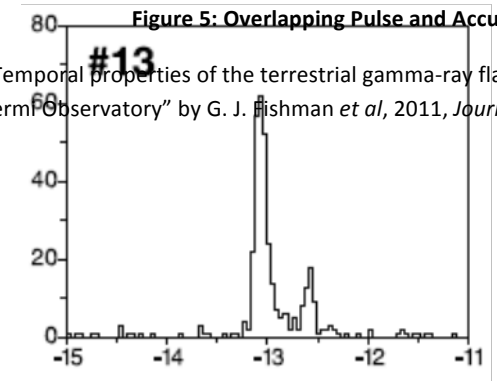

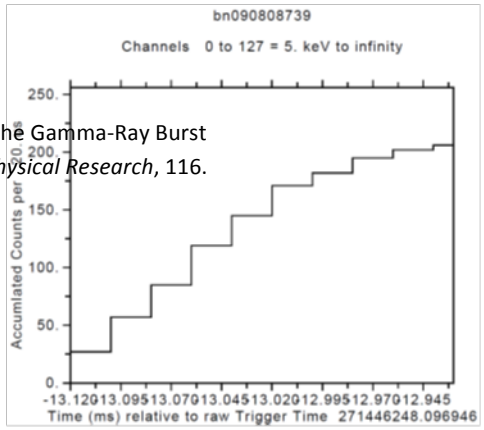

Figure 5: Overlapping Pulse and Accumulation

Reprinted from "Temporal properties of the terrestrial gamma-ray flashes from the Gamma-Ray Burst Monitor on the Fermi Observatory" by G. J. Fishman *et al*, 2011, *Journal of Geophysical Research*, 116.

Histogram of TGF **Histogram of Accumulated TGF**

Matthew Stanbro: Hartigan's Dip Test of Unimodality Applied on TGFs.

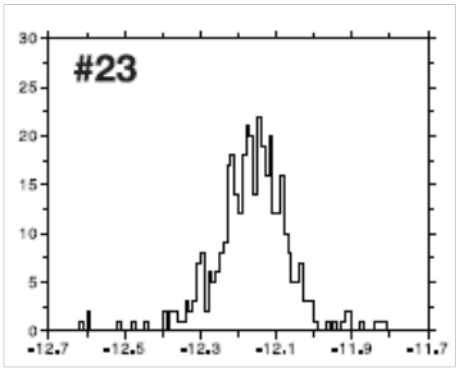

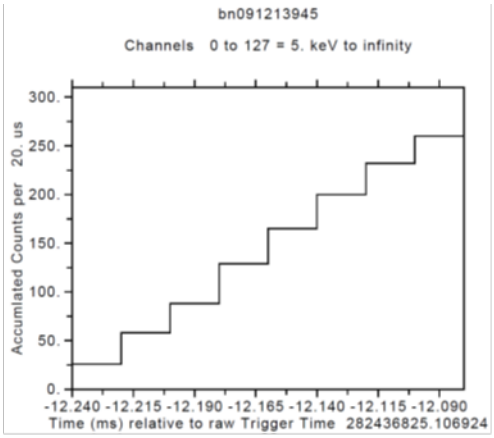

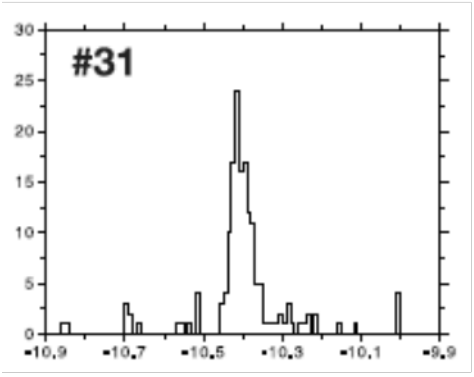

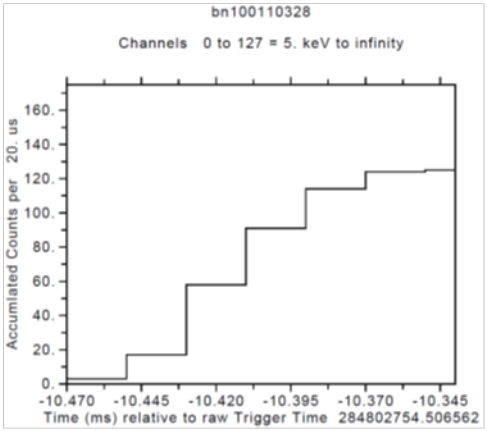

Bibliography

Briggs, M.S., Fishman, G.J., Connaughton, V., Bhat, P.N., Paciesas, W.S., Preece, R.D., … Chekhtman, A. (2010). First results on terrestrial gamma-ray flashes from the Fermi Gamma-ray Burst Monitor. *Journal of Geophysical Research – Space Physics,* 115, 14. doi: 10.1029/2009JAO15242

Fishman, G.J., Bhat, P.N., Mallozi, R., Horack, J.M., Koshut, T., Kouveliotou, C., … Christian, H.J. (1994). Discovery of intense gamma-ray flashes of atmospheric origin. *Science*, 264(5163), 1313-1316. doi: 10.1126/science.264.5163.1313

Fishman, G.J., Briggs, M.S., Connaughton, V. Bhat, P.N., Paciesas, W.S., von Kienlin, A., … Greiner, J. (2011). Temporal properties of the terrestrial gamma-ray flashes from the gamma-ray burst monitor on the Fermi observatory. *Journal of Geophysical Research – Space Physics,* 116, 17. doi: 10.1029/2010JA016084

Hartigan, J. A., & Hartigan, P. M. (1985). The dip test of unimodality. *The Annals of Statistics, 13,* 70-84. Retrieved from http://www.stat.washington.edu/wxs/Stat593-s03/Literature/hartigan85a.pdf

Hartigan, P.M. (1985). Algorithm as 217: computation of the dip statistic to test for unimodality. *Applied Statistics,* 34(3), 320-325. Retrieved from http://www.nicprice.net/diptest/Hartigan_1985_ApplStat.pdf

Lu, G., Cummer, S., Li, J., Han, F., Smith, D., & Grefenstette, B. (2011). Characteristics of broadband lightning emissions associated with terrestrial gamma ray flashes. *Journal of Geophysical Research, 116,* 1-12. doi: 10.1029/2010JA016141

Mechler, F. (2002). Modification of algorithm as 217: computation of the dip statistic to test for unimodality. Retreived from lib.stat.cmu.edu/apstat/217

Metcalf, M., Reid, J., & Cohen, M. (2004). Fortran 95/2003 explained. New York, NY: Oxford University Press Inc.

NASA (2012, March). Fermi Gamma-ray Space Telescope database, ftp://heasarc.gsfc.nasa.gov//glast/data/gbm/triggers

Smith, D. (2009). Terrestrial gamma-ray flashes, relativistic runaway, and high-energy radiation in the atmosphere. *AIP Conference Proceedings, 1118*, 34-45. doi: 10.1063/1.3137710